PII S0016-7037(02)01218-8

Extremely rapid cooling of a carbonaceous-chondrite chondrule containing very ^{16}O-rich olivine and a ^{26}Mg-excess

HISAYOSHI YURIMOTO[1],* and JOHN T. WASSON[2]

[1]Department of Earth and Planetary Sciences, Tokyo Institute of Technology, Meguro, Tokyo 152-8551, Japan
[2]Institute of Geophysics and Planetary Physics, University of California, Los Angeles, CA 90095-1567, USA

Abstract—We describe a phenocryst in a CO-chondrite type-II chondrule that we infer to have formed by melting an amoeboid olivine aggregate (AOA). This magnesian olivine phenocryst has an extremely ^{16}O-rich composition $\Delta^{17}O (=\delta^{17}O - 0.52 \cdot \delta^{18}O) = -23$‰. It is present in one of the most pristine carbonaceous chondrites, the CO3.0 chondrite Yamato 81020. The bulk of the chondrule has a very different $\Delta^{17}O$ of -1‰, thus the $\Delta^{17}O$ range within this single chondrule is 22‰, the largest range encountered in a chondrule. We interpret the O isotopic and Fe-Mg distributions to indicate that a fine-grained AOA assemblage was incompletely melted during the flash melting that formed the chondrule. Some Fe-Mg exchange but negligible O-isotopic exchange occurred between its core and the remainder of the chondrule. A diffusional model to account for the observed Fe-Mg and O-isotopic exchange yields a cooling rate of 10^5 to 10^6 K hr^{-1}. This estimate is much higher than the cooling rates of 10^1 to 10^3 K hr^{-1} inferred from furnace simulations of type-II chondrule textures (e.g. Lofgren, 1996); however, our cooling-rate applies to higher temperatures (near 1900 K) than are modeled by the crystal-growth based cooling rates. We observed a low ^{26}Al/^{27}Al initial ratio $((4.6 \pm 3.0) \cdot 10^{-6})$ in the chondrule mesostasis, a value similar to those in ordinary chondrites (Kita et al., 2000). If the ^{26}Al/^{27}Al system is a good chronometer, then chondrule I formed about 2 Ma after the formation of refractory inclusions. *Copyright © 2002 Elsevier Science Ltd*

1. INTRODUCTION

Chondrules formed by the flash melting of solid precursors in the solar nebula (Gooding et al., 1980; Wasson, 1993; Hewins, 1996; Rubin, 2000). However, the nature of the precursors and the heating/cooling processes are still unresolved issues. Furnace experiments can reproduce some textural and chemical features with cooling rates of 10^1 to 10^3 K hr^{-1} (Hewins and Radomsky, 1990; Lofgren, 1996), but other features (volatile retention, relict crystal preservation) imply much faster cooling rates (Wasson, 1996; Greenwood and Hess, 1996).

Variations of oxygen isotopic anomalies in $\Delta^{17}O$ ($=\delta^{17}O - 0.52 \cdot \delta^{18}O$) among whole chondrules from all meteorite groups are restricted from -5‰ to $+2$‰ with the ranges smaller within individual groups (Clayton et al., 1991 Rubin et al., 1990). The range in $\Delta^{17}O$ values measured in chondrule phases extends somewhat lower to -10‰ (Hiyagon, 1997; Maruyama et al., 1999; Leshin et al., 2000; Russell et al., 2000; Jones et al., 2000; Wasson et al., 2000a; 2000b). In contrast, the $\Delta^{17}O$ values among phases in refractory inclusions span a much broader range from less than ≈ -25‰ to ≈ 0‰ (Clayton, 1993).

Chondrules and refractory or calcium-aluminum-rich inclusions (CAIs) differ in their initial ^{26}Al/^{27}Al ratios; the sparse available data on (mainly ordinary-chondrite) chondrules indicate ratios that are an order of magnitude lower (Kita et al., 2000; Huss et al., 2001) than those in CAIs (MacPherson et al., 1995). If the Al in the chondrules and refractory inclusions were extracted from the same well-mixed reservoir, the chon-

drules formed ~2 Ma after the refractory inclusions. Thus, both the O-isotopic compositions and initial ^{26}Al/^{27}Al ratios indicate that chondrules had a different origin from CAIs.

The CO 3.0 chondrite Yamato 81020 (Y81020) has experienced minimal amounts of thermal metamorphism and aqueous alteration (Kojima et al., 1995). It thus preserves with great fidelity the record of processes that occurred in the solar nebula. As part of a larger study of chondrules in Y81020 we discovered that different parts of a type-II chondrule we call chondrule I had very different $\Delta^{17}O$ values. We report here our study on this chondrule. Our study offers information about the incorporation of CAI-related materials into chondrules and is interpreted to require an extremely fast cooling rate.

2. EXPERIMENTAL

2.1. Petrographic Techniques

We studied thin section Yamato 81020-56-4 from the National Institute of Polar Research (NIPR) in Tokyo. Back-scattered-electron (BSE) images of the chondrule were obtained from the C-coated section using the LEO 1430 scanning electron microscope (SEM) at the Univ. of California, Los Angeles (UCLA) and the JEOL 5310LV SEM at the Tokyo Institute of Technology (TiTech). Elemental compositions were determined using energy dispersion techniques on the SEM at TiTech (using an Oxford LINK ISIS operating system) and by using wavelength dispersion on the UCLA Cameca Camebax electron microprobe. Most of the phase composition data in Table 1 are from TiTech. Spatial distributions of forsterite contents and contours were determined using X-ray mapping of Mg and Fe on the TiTech SEM. X-ray intensities were converted to forsterite contents using calibration curve methods. The distribution of Al_2O_3 was also obtained by Al X-ray mapping.

2.2. Ion-Probe Techniques

The oxygen and magnesium isotope microanalyses were performed by secondary-ion mass spectrometry (SIMS) with the TiTech Cameca

* Author to whom correspondence should be addressed (yuri@geo.titech.ac.jp).

Table 1. Oxygen isotopic composition of chondrule I; $\delta^{17}O$ and $\delta^{18}O$ are relative to SMOW.

anal.	phase	$\delta^{17}O \pm \sigma_m$ (‰)	$\delta^{18}O \pm \sigma_m$ (‰)	$\Delta^{17}O \pm \sigma_m$ (‰)
large olivine phenocrysts				
01	Fo72	3.4 ± 2.4	3.6 ± 1.1	1.6 ± 2.6
02	Fo57	-0.1 ± 2.5	5.4 ± 1.2	-2.9 ± 2.8
03	Fo73	0.6 ± 2.5	5.0 ± 1.1	-2.0 ± 2.7
05	n.d.	5.5 ± 2.6	3.5 ± 1.0	3.6 ± 2.8
olivine phenocryst-4				
04	Fo68	-44.0 ± 2.5	-42.2 ± 1.2	-22.0 ± 2.8
06	Fo55	-3.7 ± 1.9	0.7 ± 1.2	-4.0 ± 2.2
07	Fo63	-47.0 ± 2.6	-38.9 ± 1.1	-26.8 ± 2.8
09	Fo54	0.1 ± 2.7	3.7 ± 1.1	-1.8 ± 2.9
10	Fo58	-18.1 ± 2.7	-14.4 ± 1.0	-10.6 ± 2.9
11	Fo49	-0.8 ± 2.9	8.1 ± 1.1	-5.0 ± 3.1
12	Fo60	-27.3 ± 2.7	-28.8 ± 1.2	-12.3 ± 2.9
14	Fo56	-36.9 ± 2.7	-40.6 ± 1.2	-15.7 ± 2.9
15	Fo52	-23.2 ± 2.0	-21.1 ± 1.0	-12.2 ± 2.2
16	Fo67	-26.1 ± 2.6	-28.5 ± 1.0	-11.3 ± 2.8
17	Fo55	-2.3 ± 2.2	-1.5 ± 1.0	-1.5 ± 2.4
18	Fo56	-36.5 ± 2.3	-37.6 ± 1.0	-16.9 ± 2.5
19	Fo51	-27.0 ± 2.9	-32.8 ± 1.1	-10.0 ± 3.1
20	Fo55	-6.6 ± 2.0	-2.2 ± 1.1	-5.5 ± 2.3
21	Fo77	-49.0 ± 2.3	-47.2 ± 1.2	-24.4 ± 2.6
22	Fo51	-38.4 ± 2.5	-36.7 ± 1.1	-19.3 ± 2.7
23*	Fo75	-43.9 ± 3.5	-41.0 ± 1.4	-22.6 ± 3.7
24	Fo85	-45.4 ± 3.8	-43.8 ± 1.6	-22.7 ± 4.1
mesostasis				
08	pl + cpx	-1.0 ± 2.3	4.3 ± 1.2	-3.3 ± 2.6

* ratio of olivine to interstitial phase = 7:3.

n.d.: not determined; Fo: forsterite; pl: plagioclase; cpx: clinopyroxene; σ_m: standard deviation of the mean based on statistics of secondary ion intensity

ims-1270 instrument. The analytical procedures were described earlier (Yurimoto et al., 1998; Koike et al., 1993). For the measurement of O isotopes the primary ion beam was mass-filtered positive 20-keV Cs ions; the typical spot size was 5 μm. The primary beam current was 3 pA, adjusted to obtain a count rate of $\approx 4 \cdot 10^5$ cps for negative ^{16}O ions. A normal incidence electron gun was utilized for charge compensation. Negative secondary ions corresponding to the ^{16}O tail, ^{16}O, ^{17}O, ^{16}OH and ^{18}O were analyzed at a mass resolution of ≈ 6000.

Table 2. Mg isotope composition of plagioclase in chondrule I.

anal.	comp.	$^{27}Al/^{24}Mg$ $\pm 2\sigma$	$f_{Mg} \pm 2\sigma_m$ ‰	$\delta^{26}Mg \pm 2\sigma_m$ ‰
mg06	An24	5 ± 1	-5.8 ± 1.4	0.9 ± 2.9
mg07	An37	20 ± 15	-20.9 ± 4.7	3.0 ± 7.2
mg10	An23	597 ± 70	-5.9 ± 7.4	27.9 ± 15.3
mg11_1	An24	147 ± 9	-11.0 ± 7.2	7.7 ± 13.0
mg11_2	An24	135 ± 11	-6.6 ± 2.7	2.7 ± 6.1
mg12	An30	13 ± 2	-8.2 ± 2.2	-3.4 ± 4.3
mg13	An37	22 ± 7	-8.3 ± 2.1	5.8 ± 4.2
mg14	An25	34 ± 44	-9.8 ± 2.7	2.0 ± 4.9
mg15	An25	79 ± 13	-7.6 ± 2.8	1.6 ± 5.6
mg16	An23	102 ± 37	-6.6 ± 2.9	0.8 ± 5.9
mg17_1	An23	204 ± 56	-7.6 ± 3.3	6.0 ± 7.9
mg17_2	An23	233 ± 6	-4.9 ± 5.1	4.9 ± 11.7

comp: anorthite contents of plagioclase
f_{Mg}: intrinsic mass fractionation from terrestrial value.
$\delta^{26}Mg$: deviation of the $^{26}Mg/^{24}Mg$ ratio from terrestrial value.
σ_m: standard deviation of the mean

For Mg isotopes the primary ion beam consisted of 23 keV $^{16}O^-$ ions. The beam diameter was 5 μm. Primary beam currents ranged from 30 to 60 pA and were adjusted for each run to obtain a ^{27}Al or ^{24}Mg count rate of not more than $4 \cdot 10^5$ cps. Positive secondary ions corresponding to ^{24}Mg, ^{25}Mg, ^{26}Mg and ^{27}Al were analyzed at a mass resolution of ≈ 4500. The following terrestrial values are used for the Mg isotope corrections: $^{25}Mg/^{24}Mg = 0.12663$, $^{26}Mg/^{24}Mg = 0.13932$ (Catanzaro et al., 1966).

3. RESULTS AND DISCUSSION

3.1. Petrographic Observations

Chondrule I, found in Y81020 CO3.0 chondrite thin section 56-4 from the NIPR, is a type-II (FeO-rich porphyritic) olivine chondrule; it is ~600 μm across and includes four large (>100 μm) subhedral olivine phenocrysts (Fig. 1). Plucking during polishing has produced a large (150-μm) hole near the center of the chondrite. The largest phenocryst has dimensions of 400 × 240 μm and covers 33% of the area of the chondrule. It has four long, essentially linear faces, and can be described as an irregular tetrahedron with rounding at two of the corners.

The second largest phenocryst is quite irregular in shape, particularly on the side facing the hole; it seems probable that some, perhaps 20%, of the plucked material consisted of portions of this phenocryst (the remainder was mesostasis). There are angular, 30 to 80-μm fragments near the periphery of this inclusion that seem to fit linear fracture faces on the inclusion, thus the phenocryst seems to have largely formed in a melting event that predated the one that formed the final chondrule. The third phenocryst is like the first in having a roughly polyhedral shape. It has 5 faces, 2 of which are essentially parallel. There appears to be a thin, ca. 4 to 10 μm-thick overgrowth layer on the face next to the large patch of mesostasis. There are many small olivine grains (5 to 50 μm) adjacent to these large phenocrysts

The mesostasis mainly consists of Ca-rich pyroxene (En$_{25}$Wo$_{49}$), albitic plagioclase (An$_{22 \text{ to } 40}$) and FeS. The larger three olivine phenocrysts range from Fo$_{70}$ near their centers to Fo$_{45}$ at the surface. If we assume that mesostasis was originally present in 80% of the large plucked hole, then the original modal composition of the chondrule was $\approx$80 vol.% olivine, $\approx$18% mesostasis and about $\approx$2% opaques, mainly FeS and chromite.

Phenocryst 4, a crystal clot ~100 μm across, has patches more Fo-rich (up to Fo$_{85}$) than the other phenocrysts (Fig. 2). Its forsterite content decreases towards the rim, and near most of the edge reaches Fo$_{45}$, the same as at the surfaces of the larger phenocrysts. Near the tip of a small peninsula located at the center of the right side of the phenocryst (Fig. 2b) olivine composition drops to Fo$_{34}$. The crystal clot contains a few tiny Al-rich patches whose compositions differ from those of the mesostasis. The largest patch ($\approx$3 μm across), located interstitially in the center, appears to have formed as a residual melt. Its composition is similar to a pyrope-rich garnet (SiO$_2$: 42.20, Al$_2$O$_3$: 22.00, MgO: 16.40, FeO: 7.30, MnO: 0.14, CaO: 11.40, Na$_2$O: 0.12 wt.%), but the material may be polycrystalline and the resemblance to pyrope coincidental.

The numerous small olivine phenocrysts are largely concentrated in two regions. The larger is between the edge of the chondrule and the two shorter faces of the largest phenocryst (Fig. 1). The typical grain size in this region is ~5 μm. The
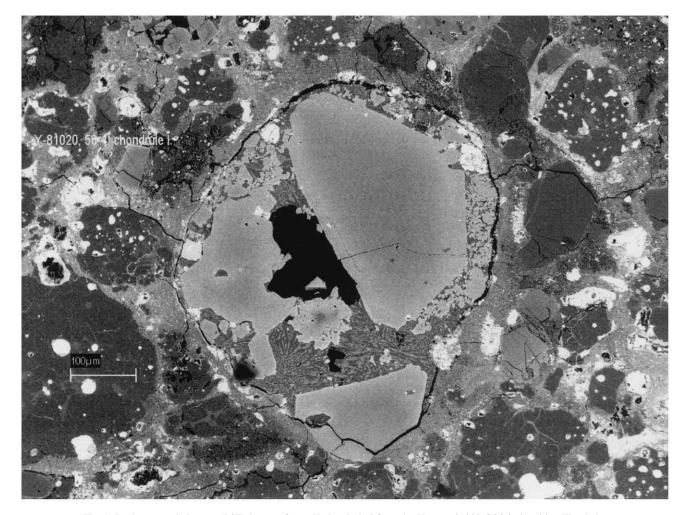
Fig. 1. Back scattered electron (BSE) image of type-II chondrule I from the Yamato 81020 CO3.0 chondrite. The dark area near the center is a plucked hole. The bulk of the chondrule consists of large (>100 μm) olivine phenocrysts with largely polyhedral shapes. The mesostasis region mainly consists of feathery Ca-pyroxene (light), plagioclase and feldspathic glass (dark). Large bright areas are either mixtures of FeS and kamacite or chromite; tiny opaques are almost all chromite. The small dimensions of the many 5 to 20 μm phenocrysts show that overgrowth layers formed after the last melting event were thin, ca. 5 μm. The ^{16}O-rich phenocryst 4 is the crystal clot just below the plucked hole.

smaller region is located near the edge of the chondrule, between the two largest phenocrysts; here the typical grain size is ~20 μm, ~4$\times$ larger than in the other region. Studies by Wasson and Rubin (2002) show that the 20 μm olivine grains have compositions ranging from Fo74 in the cores to Fo43 near the edges. The 5 μm grains have compositions ranging from Fo55 to Fo35 near the edges. Wasson and Rubin summarize different lines of evidence indicating that the maximum amount of olivine overgrowth in chondrule I following the final melting event was 8 to 10 μm, and that corrections for sectioning geometry would probably reduce these limits.

Thus it appears that the large phenocrysts are fragments of one or more olivine grains that were formed in an earlier event. The zoning partly indicates the presence of an overgrowth of new olivine during the final melting event, but igneous zoning is also preserved. The thickness of the olivine overgrowth appears to be 4 to 10 μm.

3.2. Oxygen-Isotopic Studies

The $\Delta^{17}O$ values of the four points measured on the cores of two large phenocrysts average $\approx$ 0‰; our one point on the mesostasis (Table 1 and Fig. 3) is -3‰. If we add the two highest $\Delta^{17}O$ values observed in phenocryst 4 (points 09 and 17), the seven points yield a mean of -0.9‰ and a standard deviation of 2.5‰. This is our best estimate for the mean O-isotopic composition of the high-FeO fraction of this chondrule. It is at the upper end of the range observed in chondrules from carbonaceous chondrites (Clayton, 1993; Jones et al., 2000; Wasson et al., 2000a; 2000b).

Olivine in the rim zone of phenocryst-4 has a composition of Fo$_{50}$ and $\Delta^{17}O$ values of $\approx$-2‰, similar to olivine near the surfaces of other phenocrysts and in the mesostasis. These data are consistent with crystallization of this surficial zone of phenocryst 4 from the main melt.
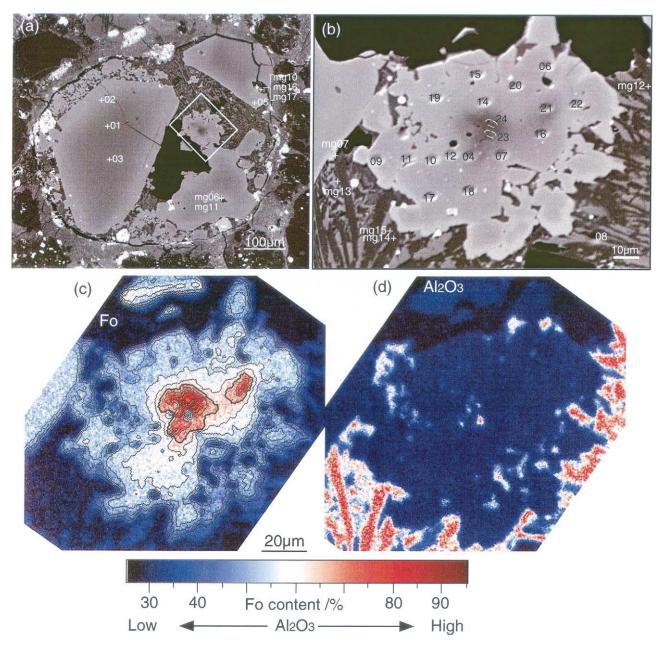
Fig. 2. Detailed BSE views and compositional contours of phenocryst 4. (a, b) Numbered craters are the sites of ion-probe analyses of oxygen; crosses mark the locations of the spots analyzed for Mg; (c) Contours of MgO/(MgO + FeO) ratios in phenocryst 4; contour lines are drawn in 5% steps from Fo_{40} to Fo_{85}. The thick line indicates the Fo_{65} level. Contour lines are partly disturbed by SIMS craters. (d) the distribution of Al_2O_3 contents in and near phenocryst 4; most Al_2O_3-rich areas are mesostasis, but one bright spot and a few tiny dots are in the Fo-rich core of phenocryst-4.

In contrast, the oxygen in the magnesian core region of phenocryst 4 (Fo>68) is ^{16}O-rich (Fig. 3); $\Delta^{17}O \approx -23‰$ (similar to values in pristine CAIs and AOAs). The lowest $\Delta^{17}O$ values are found inside the Fo_{65} contour line in Figure 2(c). This is the most ^{16}O-rich olivine ever found in a chondrule. In CO3.0 chondrite Allan Hills A77307 Jones et al. (2000) found $\Delta^{17}O$ values of $-10‰$ in a chondrule relict grain and $-9‰$ in an isolated olivine grain. The remainder of phenocryst 4 outside the Fo-rich core has intermediate O isotopic compositions; $\Delta^{17}O$ values range between -20 and

0‰. The precursors of this CO chondrule thus included olivine with a highly anomalous O-isotopic composition. For purposes of discussion, we used the $\Delta^{17}O$ values to divide phenocryst-4 into a core region $\sim 20~\mu m$ across, an intermediate zone $\sim 30~\mu m$ thick, and a rim zone $\sim 10~\mu m$ thick (Figs. 2 and 3); there is FeO zoning within and among these regions.

The tiny Al-rich mesostasis patch in the center of phenocryst 4 accounted for 30% of the area analyzed in point 23. It appears to share the same $\Delta^{17}O$ value as the core olivine, ca. $-23‰$.
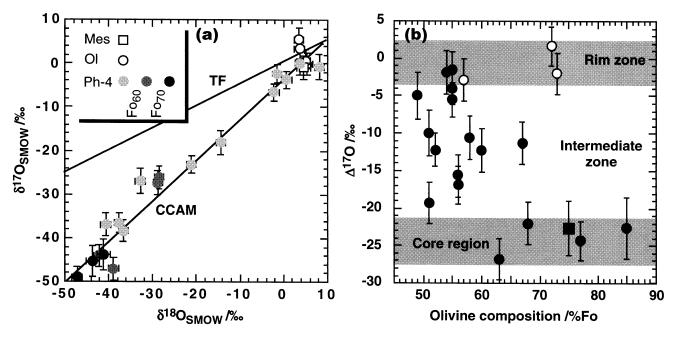
Fig. 3. Oxygen isotope distribution of major phases in chondrule I. (a) Three O-isotope diagram of major phases. Mes: mesostasis, Ol: large olivine phenocrysts, Ph-4: olivine phenocryst-4 containing ^{16}O-rich core region; shading of the solid circles indicates the forsterite content. (b) a plot of O-isotopic composition vs. forsterite content of olivine phenocrysts. Solid circle: olivine in phenocryst-4, solid rectangle: phenocryst-4 olivine plus interstitial phase, open circles: other phenocrysts. The marked zones labeled rim, intermediate and core are for phenocryst-4.

3.3. Magnesium Isotopic Compositions

We searched for spots in the chondrule mesostasis that had Al/Mg ratios high enough to allow the determination of a ^{26}Al/^{26}Mg isochron; we were able to find one anorthitic plagioclase grain with a resolvable ^{26}Mg-excess and several other grains with mean δ^{26}Mg values above the terrestrial standard (Table 2). The locations of the investigated points are shown in Figure 2. All points are taken on plagioclase, generally with a portion of the beam overlapping calcium pyroxene. With the exception of point 6, the Al/Mg ratios roughly correlate with the anorthite content of the plagioclase. Our isotopic results (Fig. 4) show a fully resolvable excess only in grain 10 which had a very high (~600) ^{27}Al/^{24}Mg ratio.

The initial ^{26}Al/^{27}Al ratio is 4.6 ± 3.0 $(2\sigma) \cdot 10^{-6}$; uncertainty limits were calculated by the York method using all measurement points. This is ~10× lower than the canonical ratio of $4.6 \cdot 10^{-5}$ commonly observed in the refractory inclusions of carbonaceous chondrites (MacPherson et al., 1995). The chondrule-I value is similar to the ratios observed in ordinary chondrites (Kita et al., 2000; Huss et al., 2001). If the ^{26}Al clock can be applied to these different materials, chondrule-I was formed 2 to 3 Ma after the formation of CAIs having an initial ^{26}Al/^{27}Al ratio of 4.6×10^{-5}. Alternatively, there may have been significant variations in the isotopic composition of Al in nebular materials, with the result that the differences in ^{26}Al/^{27}Al initial ratios cannot be simply interpreted in terms of differences in formation ages.

4. MODELING THE FORMATION OF PHENOCRYST 4

The Δ^{17}O values < -20‰ in the core of phenocryst 4 are comparable to those in olivine grains in CAIs and in pristine AOAs (Hiyagon and Hashimoto, 1999; Imai and Yurimoto, 2000; Komatsu et al., 2001). Thus the Δ^{17}O value in the core of phenocryst 4 suggests that the precursor mix of Ch-I contained an AOA or a similar olivine-rich assemblage. AOAs also commonly contain minor amounts (10 to 20% each) of Ca-Al-rich phases such as anorthite and diopside, and could thus account for the Al-rich mesostasis patch. There is one past report of a relict AOA incorporated into a chondrule (Mc-Sween, 1977).

However, the FeO content of the core of phenocryst 4 is much too high to allow the interpretation that it is a relatively unaltered AOA relict. The olivine in the least altered AOAs has very low FeO contents; Chizmadia et al. (2002) measured Fo values of 97 to 100 mol.% in CO3.0 chondrites, but inferred that the lowest values reflected contamination by iron oxides produced by terrestrial weathering and suggested that the primordial range was 99 to 100 mol.%.

We have therefore examined the processes and conditions required to form phenocryst-4 from a low-FeO AOA precursor. We considered two extreme conditions: in the first, the precursor remained as a relict and the redistributions of Fo contents occurred in the precursor without O isotopic redistribution, i.e., volume diffusion increased FeO contents of the solid olivine in the core; in the second, much of the precursor AOA melted, and the Fe-Mg and O isotopic exchanges occurred in the melt.

To evaluate these models we calculated the relationship between diffusion time, cooling rate and temperature for melts
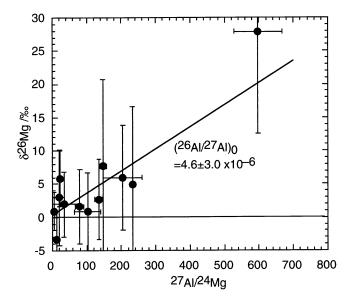
Fig. 4. ^{26}Mg-^{26}Al systematics in chondrule I. Error bars denote 2σ uncertainties of the points. Uncertainty limits of the slope are also 2σ. Point 10, with a $^{27}Al/^{24}Mg$ ratio of ≈ 600, has a $\delta^{26}Mg$ significantly higher than the terrestrial value. There are small ($\sim 2‰$) ^{26}Mg excesses in points having lower ratios (90 to 230) but uncertainty limits overlap terrestrial values. The initial $^{26}Al/^{27}Al$ ratio is $\sim 10X$ lower than the canonical ratio observed in refractory inclusions.
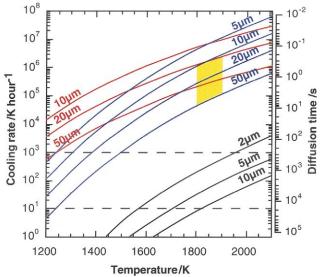

Fig. 5. Diffusion modeling. Relationships among cooling rate, temperature, diffusion time and the thickness of the diffusion zones preserved after cooling and crystallization. Blue, red, and black curves correspond to the diffusion of O and Co (a proxy for Fe and Mg) in the melt and Fe in olivine, respectively. The numbers on the lines correspond to the radial thickness of the zones limited by values representing approximately 10 and 90% changes in the initial concentration. Dashed lines correspond to upper and lower limits of chondrule cooling rates based on furnace experiments (Lofgren, 1996). The yellow area corresponds to the inferred cooling rate of chondrule I by flash heating (see text).

and solids. The radial thickness of the O- and Fe-Mg-diffusive mixing zones under flash heating conditions were evaluated by compressed-time-scale techniques (Dodson, 1973; Lasaga, 1983) using O- and Co-diffusion coefficients determined for basaltic melts (Hofmann and Magaritz, 1977; Canil and Muelenbachs, 1990) and the Fe-Mg diffusion coefficient for olivine (Chakraborty et al., 1994). We used Co diffusion data as a proxy for (the unmeasured) Fe or Mg diffusivities in the melt because it has a similar ionic charge and ionic radius (Hofmann, 1980). The initial temperature is assumed to be that at which overgrowth of olivine started in phenocryst 4.

In Figure 5 we compare the diffusion lengths, x, of O and Fe-Mg as a function of initial crystallization temperature, T_0, and cooling rate, s. Following Lasaga (1983) we put $x = 2(D_0 \cdot t')^{1/2}$ where $t' = R \cdot T_0^2 \cdot (E \cdot s)^{-1}$, R is the gas constant, E is the diffusion activation energy and D_0 the diffusion coefficient at T_0. For isothermal conditions, the radial thickness of the diffusion layers (defined by $2(D \cdot t)^{1/2}$, where D is the diffusion coefficient; t is the diffusion time) due to olivine dissolution at constant temperature were also calculated as a function of diffusion time and the temperature. Thus, the temperature axis corresponds either to the initial temperature during cooling or the temperature of dissolution.

In the first model we assumed the core region to be an intact relict AOA that, at the last, was surrounded by a melt consisting of the intermediate zone; this model required the Fe-enrichment in the core to be the product of volume diffusion into the relict olivine. To diffuse Mg 10 μm to the center of the 20 μm relict at a temperature near 1850 K (a rough estimate of the liquidus temperature for the intermediate zone) requires a duration of heating of $\sim 10^4$ to 10^5 s equivalent to a cooling rate of 2 to 20 K hr^{-1} (Fig. 5). If we assume a mean olivine grain size of only

4 μm (according to Chizmadia et al., 2002, the typical size in AOAs), with rapid diffusion along grain boundaries, diffusion exchange requires as little as 700 s or 300 K hr^{-1}. Even the latter heating duration is inconsistent with the heterogeneous $\Delta^{17}O$ distribution in the wide (the typical thickness ≈ 30 μm; the range is from 20–50 μm, Fig. 2) intermediate zone which was almost certainly molten. Diffusion during this extended thermal event would have homogenized the O-isotopic composition in this melt (Fig. 5) in <10 s or $>10^4$ K hr^{-1}.

Next we assumed that the intermediate zone and the core region were not molten during heating. In this case, the Mg-Fe and O isotopic zoning observed in these zones has been achieved by diffusion in olivine. To diffuse Mg (30 to 60 μm) to the center of the relict zone at ~ 1850 K required a cooling rate of <1 K hr^{-1}. Such slow cooling rate obtained by Mg-Fe diffusion in olivine is much slower than the estimation based on furnace experiments (Lofgren, 1996). Moreover, since O self diffusion in olivine is about four orders of magnitude slower than the Mg-Fe diffusion (Jaoul et al., 1980), the Mg-Fe zoning and O isotopic zoning observed in the zones cannot be realized by a single cooling or heating event.

The centers of the three large olivine phenocrysts have compositions $\approx Fo_{73}$; and $\Delta^{17}O$ values $\approx -2‰$. We discussed above our conclusion that these are relicts. Wasson and Rubin (2002) give a more extensive discussion.

In the phenocryst-4 crystal clot olivine cores were not in equilibrium with the initial melt (whose composition is inferred from those of the small phenocrysts). The last olivine to crystallize (at the grain surfaces) has Fo contents <40 mol.%; it

appears that the first olivine to crystallize in the final melting event was more magnesian (perhaps Fo_{55}), intermediate between the compositions at the surface and core. In phenocryst-4 $\Delta^{17}O$ values $\geq -5‰$ are only observed after the Fo content falls below 55-mol.% (Fig. 3 and Table 1), consistent with the view that the layer in equilibrium with the mesostasis was thin, probably only ≈ 5 μm thick.

In our second model we examine the possibility that much of the core of phenocryst 4 was molten when the FeO enrichment occurred. Because this olivine is more forsteritic than that in the large phenocrysts, we must answer the question of why a larger fraction melted. A reasonable answer is that the grain size was much smaller (as noted above, ≈ 4 μm) in the AOA. If, because of composition and/or temperature, the melt was not saturated in magnesian olivine, because of their high surface/volume ratios, much of the fine-grained olivine would have dissolved.

We thus suggest that a melt was created by the incomplete melting of the AOA, and that this melt was not mixed mechanically with the mesostasis melt. The high FeO content in the core olivine (relative to values in pristine AOAs) is the result of diffusional Fe-Mg exchange between two melts. The olivine reprecipitated when the temperature fell below the liquidus. The Fo content of phenocryst 4 olivine can thus not be used as a marker of the original border between the two melts. Because O diffuses more slowly that Fe and Mg, the $\Delta^{17}O$ of the core largely preserved information about the olivine precursors of phenocryst 4. This illustrates the additional petrographic information that can be obtained if O-isotopic studies are included.

The Al-rich patch of phenocryst-4 appears to have the same O-isotopic composition ($\Delta^{17}O \approx -23‰$) as the adjacent olivine (Fig. 3 and Table 1). We infer that this material originated in the AOA precursor (AOAs commonly contain 20 to 30% anorthite and diopside) and was trapped as residual melt between the boundaries of relict olivine grains. Note that the Na_2O content of this patch is only 0.12%, thus this melt is much more refractory than the mesostasis that surrounds the phenocrysts.

It seems impossible to form the intermediate zone of phenocryst 4 by a mechanism similar to that suggested by Cohen et al. (2000), the slow isothermal dissolution of an AOA relict below the liquidus temperature. To preserve the record of diffusion in the intermediate zone, the olivine must grow fast enough to prevent the homogenization of the oxygen isotopes in the 20 to 50 μm thickness of melt, which is estimated to require <10 s at 1800 K (Fig. 5). Such fast growth would imply rapid cooling at $>10^4$ $K \cdot hr^{-1}$, far in excess of that envisioned by Cohen and coworkers.

In summary, we find the compositional evidence most consistent with rapid cooling following the flash melting of the chondrule in the solar nebula. We suggest that, during this event, the mesostasis, surficial layers on the large phenocrysts and portions of the AOA olivine grains melted, but that the phenocryst-4 melt did not mechanically mix with the main chondrule melt.

In the phenocryst-4 region the first solids nucleated on the surviving unmelted AOA olivine. The composition of the intermediate zone was produced from the mixing by diffusion of elements and isotopes between the main chondrule melt and the melt in phenocryst 4. The partial preservation of anomalous O in the intermediate zone shows that the crystal growth rate of

phenocryst-4 olivine was faster than the O diffusion rate in the melt in this zone.

From information summarized by Wasson (1996) we estimate that the liquidus temperature of the intermediate zone was 1800 to 1900 K. The peak temperature in the melt may have initially been somewhat higher, but not long enough to allow complete melting of the large phenocrysts or most of the forsteritic AOA olivine. From the diffusion modeling summarized in Figure 5 we estimate that, to preserve the composition of the 30-μm thickness of the intermediate zone in the melt, the cooling rate at temperatures in the range 1800 to 1900 K needed to be greater than $\sim 10^5$ $K\ hr^{-1}$. In contrast, since only limited amounts of Fe and Mg were transferred across the intermediate zone to produce the elevated FeO contents of the core region, the upper limit of the cooling rate is estimated to be $\sim 10^6$ $K \cdot hr^{-1}$.

The resulting limits on the cooling rate of 10^5 to 10^6 $K\ hr^{-1}$ are 2 to 3 orders of magnitude larger than those estimated for type-II chondrules based on furnace experiments but consistent with the cooling rate of $10^{4\ to\ 6}$ $K\ hr^{-1}$ calculated for direct radiation of a mm-size chondrule into space (Hood and Kring, 1996; Wasson, 1996). Similarly high cooling rates have been inferred to account for the retention of volatiles such as S (Wasson, 1996).

Part of this difference is due to the fact that our cooling rates apply at temperatures 100 to 200 K higher than those for FeO-rich type-II phenocrysts (Lofgren, 1996). In chondrule I the cores of the large grains appear to be relics (it is possible that they are from the same original chondrule), and the original host chondrule may have been in an environment that cooled more slowly. However, as Wasson (1996), stated, the single-heating-event model on which the furnace-experiments are based seems to be incorrect in detail. This model requires that the texture be largely determined by single melting events. In fact, it appears that most chondrules have experienced appreciable melting several times (Rubin and Krot, 1996). And, since all chondrule melting models produce ranges of temperatures, most chondrules probably reached solidus temperatures >10 times. It is therefore essential to find additional evidence that allows the determination of cooling rates that can be uniquely ascribed to the last melting event recorded in the chondrule.

5. SUMMARY

Our study has uncovered exceptionally large ($>20‰$) variations in $\Delta^{17}O$ within a single chondrule in a primitive CO chondrite. This observation expands upon previously reported isotopic evidence indicating that refractory inclusions were incorporated into chondrules (Misawa and Nakamura, 1996; Maruyama et al., 1999; Krot et al., 1999). Materials having ^{16}O-rich and ^{16}O-poor compositions produced at different nebular places and/or different times were mixed mechanically, were gathered into mm-size aggregates, then melted to form chondrules. If $^{26}Al/^{27}Al$ ratios provide chronologic information, the last melting occurred ~ 2 Ma after the formation of refractory inclusions. The small variations in $\Delta^{17}O$ among bulk chondrules (Clayton, 1993) and chondrule phases (Hiyagon, 1997; Maruyama et al., 1999; Leshin et al., 2000; Russell et al., 2000; Jones et al., 2000; Wasson et al., 2000a, 2000b) document the high efficiency of mixing of these types of materials

but perhaps also the low abundance of refractory objects in the set of chondrule precursor materials.

REFERENCES

Canil D. and Muehlenbachs K. (1990) Oxygen diffusion in an Fe-rich basalt melt. *Geochim. Cosmochim. Acta* **54**, 2947–2951.

Catanzaro E. J., Murphy T. J., Garner E. L., and Shields W. R. (1966) Absolute isotopic abundance ratios and atomic weight of magnesium. *J. Res. Nat. Bur. Stand.* **70a**, 453–458.

Chakraborty S., Farver J. R., Yund R. A., and Rubie D. C. (1994) Mg tracer diffusion in synthetic forsterite and San Carlos olivine as a function of P, T, and fO_2. *Phys. Chem. Min.* **21**, 489–500.

Clayton R. N. (1993) Oxygen isotopes in meteorites. *Ann. Rev. Earth Planet. Sci.* **21**, 115–149.

Clayton R. N., Mayeda T. K., Goswami J. N., and Olsen E. J. (1991) Oxygen isotope studies of ordinary chondrites. *Geochim. Cosmochim. Acta* **55**, 2317–2337.

Cohen B. A., Hewins R. H., and Yu Y. (2000) Evaporation in the young solar nebula as the origin of "just-right' melting of chondrules. *Nature* **406**, 600–602.

Dodson M. H. (1973) Closure temperature in cooling geochronological and petrological systems. *Contrib. Mineral. Petrol.* **40**, 259–274.

Gooding J. L., Keil K., Fukuoka T., and Schmitt R. A. (1980) Elemental abundances in chondrules from unequilibrated chondrites: Evidence for chondrule origin by melting of pre-existing materials. *Earth Planet. Sci. Lett.* **50**, 171–180.

Greenwood J. P. and Hess P. C. (1996) Congruent melting kinetics: Constraints on chondrule formation. In *Chondrules and the Protoplanetary Disk* (ed. R. H. Hewins, R. H. Jones, and E. R. D. Scott), pp. 205–211. Cambridge University Press.

Hewins R. H. (1996) Chondrules and the protoplanetary disk: an overview. In *Chondrules and the Protoplanetary Disk* (ed. R. H. Hewins, R. H. Jones, and E. R. D. Scott), pp. 3–9. Cambridge Univ. Press.

Hewins R. H. and Radomsky P. M. (1990) Temperature conditions for chondrule formation. *Meteoritics* **25**, 309–318.

Hiyagon H. (1997) In situ analysis of oxygen isotopes and Fe/Mg ratios in olivine using SIMS: preliminary results for an Allende chondrite. *Antarct. Meteorit. Res.* **10**, 249–274.

Hiyagon H. and Hashimoto A. (1999) [16]O excesses in olivine inclusions in Yamato-86009 and Murchison chondrules and their relation to CAIs. *Science* **283**, 828–831.

Hofmann A. W. (1980) Diffusion in natural silicate melts: a critical review. In *Physics of Magmatic Processes* (ed. R. Hargraves), pp. 385–417. Princeton University Press.

Hofmann A. W. and Magaritz M. (1977) Diffusion of Ca, Sr, Ba, and Co in a basalt melt: implications for the geochemistry of the mantle. *J. Geophys. Res.* **82**, 5432–5440.

Hood L. L. and Kring D. A. (1996) Models for multiple heating mechanisms. In *Chondrules and the Protoplanetary Disk* (ed. R. H. Hewins, R. H. Jones, and E. R. D. Scott), pp. 265–276. Cambridge University Press.

Huss G. R., MacPherson G. J., Wasserburg G. J., Russell S. S., and Srinivasan G. (2001) Aluminum-26 in calcium-aluminum-rich inclusions and chondrules from unequilibrated ordinary chondrites. *Meteorit. Planet. Sci.* **36**, 975–997.

Imai H. and Yurimoto H. (2000) Distribution of oxygen isotopes in an amoeboid olivine aggregate from the Allende meteorite. (abstract). *Antarct. Meteorit.* **25**, 29–31.

Jaoul O., Froidevaux C., Durham W. B., and Michaut M. (1980) Oxygen self-diffusion in forsterite: Implications for the high-temperature creep mechanism. *Earth Planet. Sci. Lett.* **47**, 391–397.

Jones R. H., Saxton J. M., Lyon I. C., and Turner G. (2000) Oxygen isotopes in chondrule olivine and isolated olivine grains from the CO3 chondrite, ALHA77307. *Meteorit. Planet. Sci.* **35**, 849–857.

Kita N. T., Nagahara H., Togashi S., and Morishita Y. (2000) A short duration of chondrule formation in the solar nebula: Evidence from [26]Al in Semarkona ferromagnesian chondrules. *Geochim. Cosmochim. Acta* **64**, 3913–3922.

Koike O., Yurimoto H., Nagasawa H., and Sueno S. (1993) Ion microprobe measurements of Mg isotopes in Type B1 CAI of Allende meteorite. *Proc. NIPR Symp. Antarct. Meteorites.* **6**, 357–363.

Kojima T., Yada S., and Tomeoka K. (1995) Ca-Al-rich inclusions in three Antarctic CO3 chondrites, Yamato-81020, Yamato-82050, and Yamato-790992: Record of low-temperature alteration. *Proc. NIPR Symp. Antarct. Meteorit.* **8**, 79–96.

Komatsu M., Krot A. N., Petaev M. I., Ulyanov A. A., Keil K., and Miyamoto M. (2001) Mineralogy and petrography of amoeboid olivine aggregates from the reduced CV3 chondrites Efremovka, Leoville and Vigarano: Products of nebular condensation, accretion and annealing. *Meteorit. Planet. Sci.* **36**, 629–641.

Krot A. N., Sahijpal S., McKeegan K. D., Weber D., Greshake A., Ulyanov A. A., Hutcheon I. D., and Keil K. (1999) Mineralogy, aluminum-magnesium-isotopic, and oxygen-isotopic studies of the relic calcium-aluminum-rich inclusions in chonrules (abstract). *Meteorit. Planet. Sci.* **34**, A68–69.

Lasaga A. C. (1983) Geospeedometry: an extension of geothermometry. In *Kinetics and Equilibrium in Mineral Reactions* (ed. S. K. Saxena), pp. 81–114. Springer-Varlag.

Leshin L. A., McKeegan K. D., Benedix G. K. (2000) Oxygen isotope geochemistry of olivine from carbonaceous chondrites. (abstract). *Lunar Planet. Sci.* **31**, abs.1918. (CD-ROM).

Lofgren G. E. (1996) A dynamic crystallization model for chondrule melts. In *Chondrules and the Protoplanetary Disk* (ed. R. H. Hewins, R. H. Jones, and E. R. D. Scott), pp. 187–196. Cambridge University Press.

MacPherson G. J., Davis A. M., and Zinner E. K. (1995) The distribution of aluminum-26 in the early solar system- a reappraisal. *Meteoritics* **30**, 365–386.

Maruyama S., Yurimoto H., and Sueno S. (1999) Oxygen isotope evidence regarding the formation of spinel-bearing chondrules. *Earth Planet. Sci. Lett.* **169**, 165–171.

McSween H. Y. (1977) Petrographic variations among carbonaceous chondrites of the Vigarano type. *Geochim. Cosmochim. Acta* **41**, 1777–1790.

Misawa K. and Nakamura N. (1996) Origin of refractory precursor components of chondrules from carbonaceous chondrites. In *Chondrules and the Protoplanetary Disk* (ed. R. H. Hewins, R. H. Jones, and E. R. D. Scott), pp. 99–105. Cambridge University Press.

Rubin A. E. (2000) Petrologic, geochemical and experimental constraints on models of chondrule formation. *Earth Sci. Rev.* **50**, 3–27.

Rubin A. E. and Krot A. N. (1996) Multiple heating of chondrules. In *Chondrules and the Protoplanetary Disk* (ed. R. H. Hewins, R. H. Jones, and E. R. D. Scott), pp. 173–180. Cambridge University Press.

Rubin A. E., Wasson J. T., Clayton R. N., and Mayeda T. K. (1990) Oxygen isotopes in chondrules and coarse-grained chondrule rims from the Allende meteorite. *Earth Planet. Sci. Lett.* **96**, 247–255.

Russell S. S., Lyon I., Saxton J. (2000). Oxygen isotope microanalysis of an Allende compound chondrule (abstract). *Lunar Planet. Sci.* **31**, Abs.1949. (CD-ROM).

Wasson J. T. (1993) Constraints on chondrule origins. *Meteoritics* **28**, 14–28.

Wasson J. T. (1996) Chondrules formation energetics and length scales. In *Chondrules and the Protoplanetary Nebula* (ed. R. H. Hewins, R. Jones, and E. R. D. Scott), pp. 45–51. Cambridge University Press.

Wasson J. T., Kallemeyn G. W., and Rubin A. E. (2000a) Chondrules in the LEW85332 ungrouped carbonaceous chondrite: Fractionation processes in the solar nebula. *Geochim. Cosmochim. Acta* **64**, 1279–1290.

Wasson J. T., Rubin A. E., and Yurimoto H. (2000b) CO chondrule evidence for a drift in the nebular oxygen-isotopic composition (abstract). *Meteorit. Planet. Sci.* **35,** A166–167.

Yurimoto H., Ito M., and Nagasawa H. (1998) Oxygen isotope exchange between refractory inclusions in Allende and solar nebula gas. *Science* **282,** 1874–1877.

Chizmadia L. J., Rubin A. E., and Wasson J. T. (2002). Mineralogy and petrology of amoeboid olivine inclusions: Evidence for CO3 parent-body aqueous alteration. *Meteorit. Planet. Sci.* **35,** in press.

Wasson J. T. and Rubin A. E. (2002). Ubiquitous relict grains in type-II chondrules, narrow overgrowths, and chondrule cooling rates following the last melting event. Lunar Planet Sci. (abstract) 1141 pdf.